Editors' Suggestion

Particle-Hole Symmetry and the Fractional Quantum Hall Effect in the Lowest Landau Level

W. Pan,[1,2,3] W. Kang,[4] M. P. Lilly,[3] J. L. Reno,[3] K. W. Baldwin,[5] K. W. West,[5] L. N. Pfeiffer,[5] and D. C. Tsui[5]
[1]Materials Physics Department, Sandia National Laboratories, Livermore, California 94551, USA
[2]Quantum Phenomena Department, Sandia National Laboratories, Albuquerque, New Mexico 87185, USA
[3]Center for Integrated Nanotechnologies, Sandia National Laboratories, Albuquerque, New Mexico 87185, USA
[4]Department of Physics, University of Chicago, Chicago, Illinois 60637, USA
[5]Department of Electrical Engineering, Princeton University, Princeton, New Jersey 08544, USA

(Received 19 March 2019; revised manuscript received 14 December 2019; accepted 19 March 2020; published 15 April 2020)

We report on detailed experimental studies of a high-quality heterojunction insulated-gate field-effect transistor (HIGFET) to probe the particle-hole symmetry of the fractional quantum Hall effect (FQHE) states about half-filling in the lowest Landau level. The HIGFET is specially designed to vary the density of a two-dimensional electronic system under constant magnetic fields. We find in our constant magnetic field, variable density measurements that the sequence of FQHE states at filling factors $\nu = 1/3, 2/5, 3/7\ldots$ and its particle-hole conjugate states at filling factors $1\text{-}\nu = 2/3, 3/5, 4/7\ldots$ have a very similar energy gap. Moreover, a reflection symmetry can be established in the magnetoconductivities between the ν and $1\text{-}\nu$ states about half-filling. Our results demonstrate that the FQHE states in the lowest Landau level are manifestly particle-hole symmetric.

DOI: 10.1103/PhysRevLett.124.156801

The fractional quantum Hall effect (FQHE) [1] found in a two-dimensional electron system (2DES) under low temperatures and high magnetic fields is a unique, emergent state of matter with remarkable properties. As an incompressible quantum fluid of electrons, some of the exotic properties of the FQHE include fractional charge [2], anyonic excitations [3–5], and non-Abelian statistics [6,7]. There has been considerable interest in the realization of fault tolerant topological quantum computing to take advantage of the anyonic excitation in the FQHE [8,9].

Historically, the most successful approach toward understanding the FQHE and related phenomena was based on the theory of Halperin, Lee, and Read (HLR) [10], which maps the electrons at half-filled Landau level to a system of composite fermions coupled to a Chern-Simons gauge field [11,12]. Such a singular gauge transformation serves to attach two flux quanta of magnetic field on the average to every electron, leading to a system of composite fermions that moves under a zero effective magnetic field at half-filling. The FQHE states at filling factors $\nu = p/(2p \pm 1)$, where $p = 1, 2, 3\ldots$, can be understood as $\nu^* = p$ integer quantum Hall effect states of composite fermions. Here, $\nu = nh/eB$. n is the 2DES density, h the Planck constant, e the electron charge, and B the magnetic field.

Over the years, experiments have provided strong support for the existence of composite fermions at half-filling [13–16]. In turn, the composite fermion theory has been a very successful as a consistent framework to understand the experiments on the FQHE. Recently, particle-hole symmetry (PHS) in the lowest Landau level [17] has generated renewed interest in the physics of composite fermions at half-filling [18–30]. The HLR theory has largely neglected the presence of particle-hole symmetry even though a two-dimensional electronic system with a partially filled Landau level of spin-polarized electrons possesses an exact PHS about half-filling in the limit of zero effective mass.

In an approach that is distinct from the HLR theory, a new theory has conjectured that the composite fermions (CFs) at half-filled Landau level may be a Dirac particle [21]. As an effective theory of composite fermions at half-filling, the Dirac composite fermion theory shares a number of predictions about the experiments with the HLR theory. Since a Dirac particle possesses an inherent PHS about half-filling, the PHS in a Dirac composite fermion theory is explicit. Support for the Dirac composite fermion theory has come from studies of numerics. However, there is a general lack of understanding of how the Dirac theory of composite fermions may emerge from the microscopics starting from a Hamiltonian for two-dimensional electrons. It also remains unclear how the Dirac theory of composite fermions may be distinguished experimentally from the HLR theory. We emphasize here that it is *not* the intention of this work to make a distinction between different CF pictures, though this remains a very important unresolved issue. Moreover, because different CF pictures are able to make the very same experimental predictions, it has become quite difficult to experimentally differentiate between them.

In light of these developments in the theory of CFs, experimental clarification of PHS of FQHE is necessary.

Although the PHS between the ν and 1-ν FQHE states is often taken for granted, a *direct* experimental confirmation of PH symmetry has not been made to date. Since most modulation doped GaAs/AlGaAs heterostructures have a constant density of carriers, experimental study of the ν and 1-ν FQHE states in a constant density specimen necessitates measurements at different magnetic fields. Previous experiments on constant density systems have only indirectly probed the PHS between the ν and 1-ν FQHE states in the lowest Landau level [31,32]. Their interpretations are also complicated by the energy gaps being modified by variations in the wave function, magnetic length, the Landau level mixing, and the effect of disorder potential as magnetic field is varied.

We have carried out detailed experimental studies of electronic transport properties in a specially designed heterojunction insulated-gate field-effect transistor (HIGFET) [33] in GaAs/AlGaAs heterostructures to probe the PHS between the FQHE states about the half-filling. In our experiment, we are able to measure and compare the energy gaps (E_g) of the FQHE states at ν and 1-ν at the same magnetic field, allowing for a direct comparison of the PH-symmetric FQHE states in the lowest Landau level.

Figure 1(a) shows schematically the device structure of a HIGFET used in this study. A heavily n-doped GaAs gate layer above a molecular-beam-epitaxy- (MBE) grown AlGaAs insulating layer enables a realization of uniform, high mobility 2DES as a function of the gate voltage. Figure 1(b) shows the magnetoresistance ρ_{xx} traces as a function of the electron density n in HIGFET A, measured at a fixed magnetic field of 6 T and at four separate temperatures. Well-developed FQHE states are found at the fillings $\nu = 1/3,\ 2/5,\ 3/7$, and $4/9$ for $\nu < 1/2$ and $\nu = 2/3,\ 3/5,\ 4/7$, and $5/9$ for $\nu > 1/2$. The energy gap E_g of these FQHE states is obtained from the exponential dependence of ρ_{xx} as a function of the temperature: $\rho_{xx} \sim \exp(-E_g/k_B T)$. Arrhenius plots of the three strongest FQHE states above and below $\nu = 1/2$ are shown in Fig. 1(c). Semilog plots of ρ_{xx} as a function of $1/T$ for each of the FQHE states at fillings ν and 1-ν overlap almost perfectly. This demonstrates that the conjugate pair states at filling states ν and 1-ν have essentially the same energy gap, as required by PHS. Their overlaps also imply that the disorder broadening for the ν and 1-ν states is nearly the same and particle-hole symmetric. From the slope of the linear fit, the energy gaps of the FQHE states can be obtained.

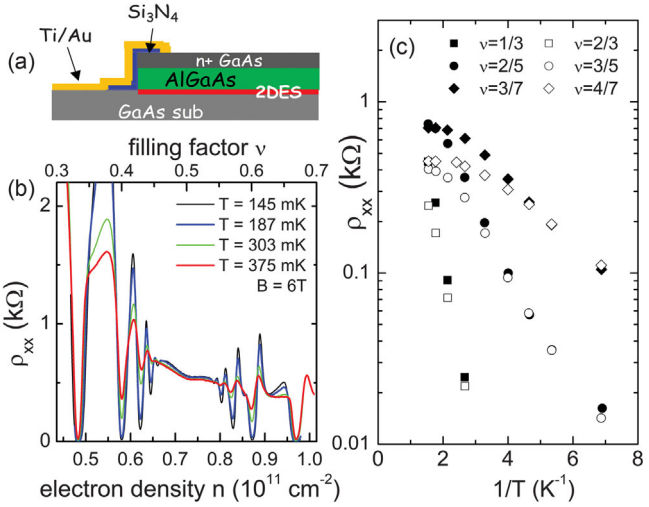

FIG. 1. (a) Schematic of the MBE device structure of a HIGFET used in this study is shown. A heavily n-doped GaAs gate layer above a MBE-grown AlGaAs insulating layer enables a realization of uniform, high mobility 2DES as a function of the gate voltage. (b) Magnetoresistance ρ_{xx} trace as a function of the electron density in HIGFET A measured at a fixed magnetic field of 6 T. The corresponding values of Landau level filling factors are shown at the top. (c) Arrhenius plots of the three strongest FQHE states above and below $\nu = 1/2$.

We have undertaken extensive temperature-dependent measurements of ρ_{xx} at other magnetic fields, data at $B = 4.5,\ 9$, and 13.5 T shown in Fig. S1 in the Supplemental Material [34]. In all cases, we find that the pairs of FQHE states at fillings ν and 1-ν states have very similar energy gaps. The variation is within 10% or less, as long as the magnetic field is the same.

To further elucidate our energy gap measurements, all the energy gap values of the FQHE states in the lowest Landau level can be compared quantitatively with theoretical predictions. The energy gaps for the pair of ν and 1-ν FQHE states are predicted to be [10]

$$E_g(\upsilon) = \frac{g^*}{|2p+1|}\frac{e^2}{\varepsilon l_B}, \tag{1}$$

where the constant $g^* = g^{\nu}$ for $\nu < 1/2$ and $g^* = g^{1-\nu}$ for $\nu > 1/2$, $p = \pm 1, \pm 2, \pm 3\ldots$, $\varepsilon = 12.8$ is the dielectric constant of GaAs, and $l_B = (h/eB)^{1/2}$ is the magnetic length. For $\nu < 1/2$, p is a positive integer; for $\nu > 1/2$, p is a negative integer. PHS requires that $g^{\nu} = g^{1-\nu}$, and the energy gaps of the ν and 1-ν states must be equal under a constant magnetic field.

Figure 2 shows the measured energy gap E_g vs $B^{1/2}/(2p+1)$ illustrating a universal scaling of the two sets of energy gap values on either side of $\nu = 1/2$ into a set of symmetric lines about the vertical with nearly equal but opposite slope. A high level of reflection symmetry about $B^{1/2}/(2p+1) = 0$ is a direct consequence of PHS about $\nu = 1/2$ [36].

We find that empirically $g^* \approx 0.15$ for both left and right sides, approximately one-half of the predicted value [10]. The reduction in the value of g^* relative to the predicted value is generally attributed primarily to the effect of finite thickness of the 2DES [37–39].

Because of disorder broadening of the energy gap of the FQHE states, we find that Eq. (1) is modified by a negative

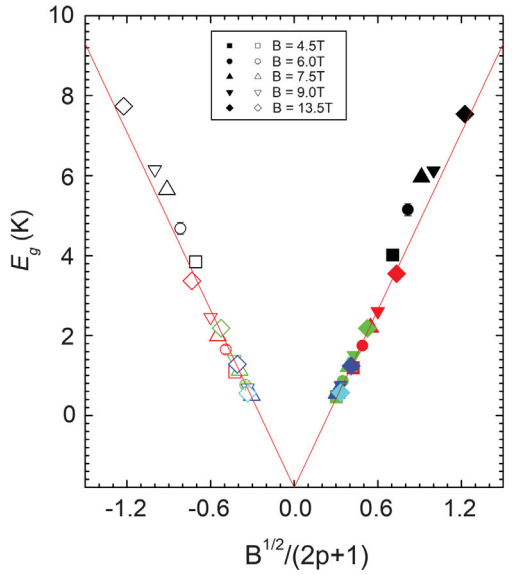

FIG. 2. Energy gaps E_g of FQHE states vs $B^{1/2}/(2p+1)$ measured at various magnetic fields. The solid symbols are for $\nu < 1/2$ and open symbols are for $\nu > 1/2$. The black color represents the third states (1/3 and 2/3), red the fifth states (2/5 and 3/5), green the seventh states (3/7 and 4/7), blue the ninth states (4/9 and 5/9), and cyan the 11th states (5/11 and 6/11). Error bars are included for the data points of $B = 6$ T. However, they are generally not visible as the size of error bars is either comparable or within the size of the symbols. The universal scaling of the energy gap values on either side of $\nu = 1/2$ is indicated by a set of symmetric lines (red color) about the vertical with nearly equal but opposite slope. The data points for the energy gaps of the 1/3 and 2/3 states are not included in the data fitting.

intercept Γ_υ with $E_g(\upsilon) = [g^*/(|2p+1|)](e^2/\varepsilon l_B) - \Gamma_\upsilon$ and $\Gamma_\upsilon \sim 1.8$ K. We also find that the effect of disorder is particle-hole symmetric with $\Gamma_\upsilon = \Gamma_{1-\upsilon}$. The existence of the disorder broadening in the energy gap energy has been observed in the past studies of the FQHE energy gap [32,40,41]. Similar disorder broadening is observed despite very different mobilities and the type of carriers. This seems to suggest that this disorder broadening is independent of the residual disorder experienced by the underlying electrons or holes. This is a perplexing phenomenon that still needs an explanation [42].

We note a slight difference of the energy gaps for the $\nu = 1/3$ and 2/3 FQHE states may be attributed to the skyrmions observed in the 1/3 FQHE state [43] and merits a further investigation. Since the energy gaps of the FQHE states can be interpreted as the effective cyclotron energy of composite fermions [10], the same slopes above and below $\nu = 1/2$ also indicate that the effective mass is the same for both the particle and hole states of CFs in the lowest Landau level. Indeed, the effective cyclotron energy of CFs can be written as $heB_{\rm eff}/m^*$ [10] where $B_{\rm eff}$ is the effective magnetic field of composite fermions, and m^* is the effective mass of composite fermions with $m^* \propto B^{1/2}$ [10]. Under a constant magnetic field, $B_{\rm eff} = B/(2p+1)$ at fillings of $\nu = p/(2p+1)$. It follows that the cyclotron energy of CFs $\propto B^{1/2}/(2p+1)$. From the values of the g^*, we obtain an effective mass of $m^* \approx 0.2m_e$, which is consistent with the effective mass obtained in previous studies in fixed density 2DES samples [40,41].

One physical parameter that may affect the energy gap of the FQHE states is the Landau level mixing, which mixes states in the lowest Landau level with those from higher lying Landau levels. The degree of Landau level mixing κ is parametrized by the ratio of Coulomb energy (which is proportional to $B^{1/2}$) over Landau level separation (which is proportional B). For example, $\kappa = 1.2$ at $B = 4.5$ T and $\kappa = 0.7$ at 13.5 T. The scaling of the energy gap data at various magnetic fields in Fig. 2 suggests that the Landau level mixing effect is expected to play a minor role in affecting the excitation gaps at ν and 1-ν [44].

In addition to the energy gap data, other evidence of the PHS of the FQHE comes from an unexpected reflection symmetry of magnetotransport coefficients between the regions of $\nu < 1/2$ and $\nu > 1/2$. In standard transport theories, such as in Boltzmann's linear response theory or in the Kubo formalism, conductivities are the direct outcomes of a diffusive transport [45]. In order to reveal PHS, one needs to convert magnetoresistivity and Hall resistivity (experimentally measured, shown in Fig. S2 of the Supplemental Material [34]) to magnetoconductivity σ_{xx} and Hall conductivity σ_{xy}, using the formula $\sigma_{xx} = \rho_{xx}/(\rho_{xx}^2 + \rho_{xy}^2)$ and $\sigma_{xy} = \rho_{xy}/(\rho_{xx}^2 + \rho_{xy}^2)$.

Figures 3(a) and 3(b) show, respectively, σ_{xx} and σ_{xy} in another HIGFET, as a function of the Landau level filling at a fixed B field of 6 T. Examining the $\sigma_{xx}(\nu)$ trace carefully, the whole trace is remarkably symmetric around $\nu = 1/2$. In fact, the reflection symmetry is clearer about the 1/2 state if the σ_{xx} trace is reversed and overlaid on top of itself. As shown in Fig. 3(c), σ_{xx} above $\nu > 1/2$ overlaps almost perfectly with σ_{xx} above $\nu < 1/2$ and vice visa. This overlap explicitly demonstrates PHS between the particle-hole conjugate ν and 1-ν FQHE states. Having revealed the unexpected reflection symmetry in σ_{xx}, we now turn to σ_{xy}. In Fig. 3(d), traces of $\sigma_{xy}(\nu)$ and 1-σ_{xy}(1-ν) are compared in Fig. 3(d). The two curves overlap very well, particularly in the gapped FQHE states.

However, the overlap is not perfect with slight discrepancy between some σ_{xx} peaks such as those found between $\nu = 1/3$ and 2/5 and between 2/3 and 3/5. The minimum between the 2/3 and 3/5 states does not occur at its PH conjugate position between 1/3 and 2/5. This minimum is probably due to a developing $\nu = 7/11$ state, which has also been observed in single junction samples of similar electron mobility before [46]. Its particle-hole conjugate state, the 4/11 state [47,48], is known to be very fragile and only exists in ultrahigh mobility wide quantum well samples. It follows that the smallness of the energy gaps for

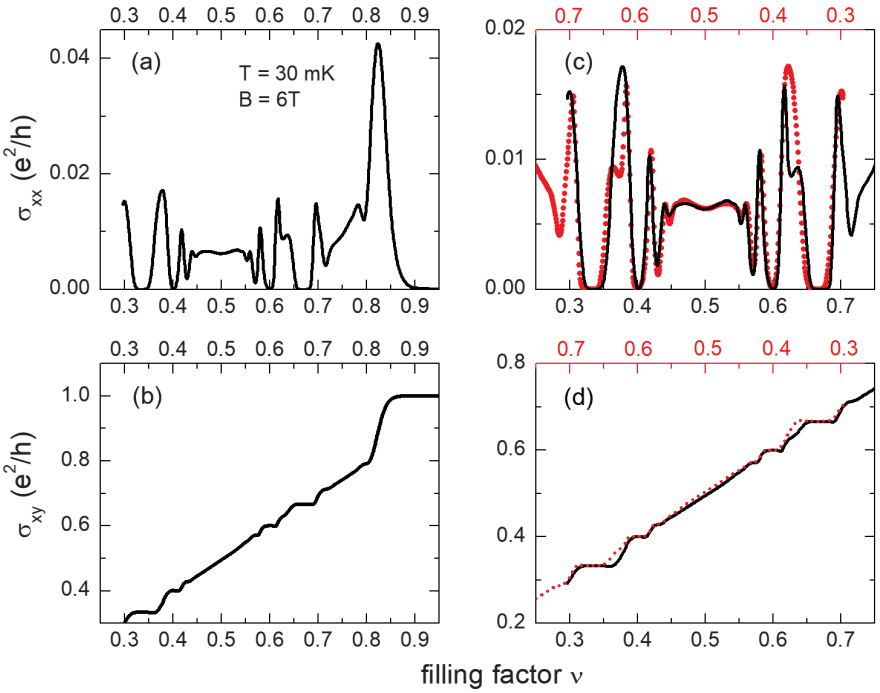

FIG. 3. (a) Longitudinal conductivity σ_{xx} converted from the measured resistivities ρ_{xx} and ρ_{xy}, around $\nu = 1/2$ at $B = 6$ T. (b) Hall conductivity σ_{xy} converted from the measured resistivities ρ_{xx} and ρ_{xy}, around $\nu = 1/2$ at $B = 6$ T. (c) Reflection symmetry in σ_{xx} about the $1/2$ state where the σ_{xx} trace is reversed (red dotted curve) and overlaid on top of itself (black curve). The top x axis shows the Landau level filling factors for the reversed curve (in red color). (d) Reflection symmetry in σ_{xy} about the $1/2$ state where the $\sigma_{xy}(\nu)$ trace (black curve) and the $1\text{-}\sigma_{xy}(1\text{-}\nu)$ trace (red dotted curve) overlap each other. The top x axis shows the Landau level filling factors for the $1\text{-}\sigma_{xy}(1\text{-}\nu)$ trace (in red color).

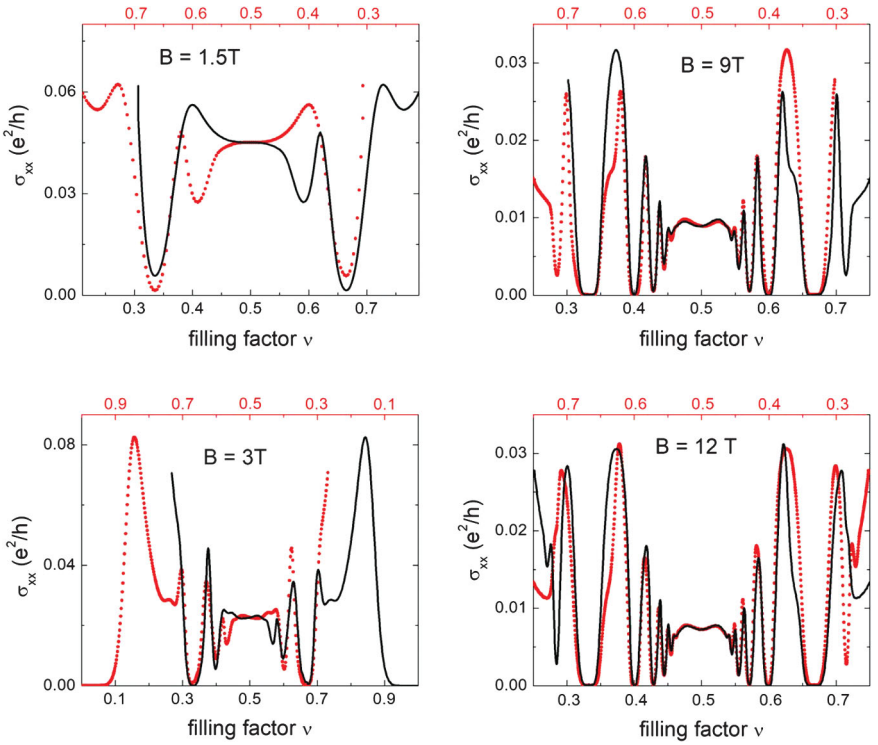

FIG. 4. Examination of reflection symmetry in σ_{xx} over a large range of magnetic fields from 1.5 to 12 T. The top x axis shows the Landau level filling factors for the reversed curves (in red color).

the $\nu = 4/11$ and $7/11$ states makes it difficult to compare fully formed states in our sample.

Figure 4 shows an evolution of the reflection symmetry in σ_{xx} over a range of magnetic fields from 1.5 to 12 T. σ_{xx} in lower magnetic fields is complicated by a stronger Landau level mixing effect as well as spin transitions. Under 1.5 T (where $\kappa = 2.1$) a large difference in σ_{xx} can be found between the ν and 1-ν states. Reflection symmetry is fully realized at larger magnetic field where the energy gaps of the FQHE states are larger and the effect of Landau level mixing may be negligibly small. We note that reflection symmetry cannot be observed in magnetic field sweeps in the constant density sample.

We add in passing that experimental results that support PHS have also been observed at fixed magnetic field experiments in single layer graphene [49–55]. In particular, experiments in Refs. [51,54,55] reported energy gap studies similar to our result in Figs. 1(c) and 2. Moreover, magnetoconductivity σ_{xx} data in Refs. [54,55], chemical potential data in Ref. [50], and capacitance data in Refs. [52,53] are also suggestive of reflection symmetry in graphene. These results demonstrate that PHS of the FQHE is likely to be universal for different material platforms. On the other hand, there are some notable differences between the FQHE found, respectively, in GaAs/AlGaAs and graphene. A disorder broadening on the order of $\sim$10 K is deduced of CFs at $\nu = 1/2$ in graphene [54,55]. This value is much larger than the $\sim$2 K observed in GaAs/AlGaAs. Another difference lies in the effective mass of CFs. A CF effective mass $m^* \approx 0.05\ m_e$ is deduced around $\nu = 1/2$ in graphene [55], while in GaAs/AlGaAs $m^* \approx 0.2\ m_e$. The difference in the dielectric constant alone cannot explain these differences and further studies are warranted.

In conclusion, we have explored the particle-hole symmetry of the FQHE in the lowest Landau level of a 2DES. We have observed nearly identical energy gaps of the FQHE states at fillings $\nu = 1/3, 2/5, 3/7\ldots$ and their particle-hole conjugate states at 1-$\nu = 2/3, 3/5, 4/7\ldots$ We have also observed a striking reflection symmetry in the magnetoconductivities between the ν and 1-ν states about half-filling. Our results have demonstrated that particle-hole symmetry is a fundamental property of the FQHE states in the lowest Landau level.

We thank K. Yang and P. A. Sharma for helpful discussions. This work was supported by a Laboratory Directed Research and Development project at Sandia National Laboratories. Materials growth and device fabrication at Sandia was supported by U.S. Department of Energy (DOE), Office of Science, Basic Energy Sciences, Materials Sciences and Engineering Division and performed at the Center for Integrated Nanotechnologies, an Office of Science User Facility operated for the DOE Office of Science. Sandia National Laboratories is a multimission laboratory managed and operated by National Technology and Engineering Solutions of Sandia, LLC., a wholly owned subsidiary of Honeywell International, Inc., for the U.S. Department of Energy's National Nuclear Security Administration under Contract No. DE-NA-0003525. This paper describes objective technical results and analysis. Any subjective views or opinions that might be expressed in the paper do not necessarily represent the views of the U.S. Department of Energy or the United States Government. Part of our measurements were performed at the National High Magnetic Field Laboratory, which is supported by the NSF Cooperative Agreement No. DMR 1157490, by the State of Florida, and the DOE. The work at University of Chicago was supported in part by the NSF EAGER. Sample growth and device fabrication at Princeton was funded by the Gordon and Betty Moore Foundation through the EPiQS Initiative No. GBMF4420, and by the National Science Foundation MRSEC Grant No. DMR-1420541.

[1] D. C. Tsui, H. L. Stormer, and A. C. Gossard, Phys. Rev. Lett. **48**, 1559 (1982).
[2] R. B. Laughlin, Phys. Rev. Lett. **50**, 1395 (1983).
[3] F. Wilczek, Phys. Rev. Lett. **49**, 957 (1982).
[4] B. I. Halperin, Phys. Rev. Lett. **52**, 1583 (1984).
[5] D. Arovas, J. R. Schrieffer, and F. Wilczek, Phys. Rev. Lett. **53**, 722 (1984).
[6] G. Moore and N. Read, Nucl. Phys. **B360**, 362 (1991).
[7] X.-G. Wen, Phys. Rev. Lett. **66**, 802 (1991).
[8] A. Y. Kitaev, Ann. Phys. (Amsterdam) **303**, 2 (2003).
[9] S. D. Sarma, M. Freedman, and C. Nayak, Phys. Rev. Lett. **94**, 166802 (2005).
[10] B. I. Halperin, P. A. Lee, and N. Read, Phys. Rev. B **47**, 7312 (1993).
[11] J. K. Jain, Phys. Rev. Lett. **63**, 199 (1989).
[12] A. Lopez and E. Fradkin, Phys. Rev. B **44**, 5246 (1991).
[13] R. L. Willett, R. R. Ruel, K. W. West, and L. N. Pfeiffer, Phys. Rev. Lett. **71**, 3846 (1993).
[14] W. Kang, H. L. Stormer, L. N. Pfeiffer, K. W. Baldwin, and K. W. West, Phys. Rev. Lett. **71**, 3850 (1993).
[15] V. J. Goldman, B. Su, and J. K. Jain, Phys. Rev. Lett. **72**, 2065 (1994).
[16] J. H. Smet, D. Weiss, R. H. Blick, G. Lütjering, K. von Klitzing, R. Fleischmann, R. Ketzmerick, T. Geisel, and G. Weimann, Phys. Rev. Lett. **77**, 2272 (1996).
[17] S. M. Girvin, Phys. Rev. B **29**, 6012(R) (1984).
[18] L. W. Wong, H. W. Jiang, and W. J. Schaff, Phys. Rev. B **54**, R17323(R) (1996).
[19] S. A. Kivelson, D.-H. Lee, Y. Krotov, and J. Gan, Phys. Rev. B **55**, 15552 (1997).
[20] D. Kamburov, Y. Liu, M. A. Mueed, M. Shayegan, L. N. Pfeiffer, K. W. West, and K. W. Baldwin, Phys. Rev. Lett. **113**, 196801 (2014).
[21] D. T. Son, Phys. Rev. X **5**, 031027 (2015).
[22] M. Barkeshli, M. Mulligan, and M. P. A. Fisher, Phys. Rev. B **92**, 165125 (2015).
[23] J. Alicea, Journal Club for Condensed Matter, http://www.condmatjclub.org/?p=2655.

[24] S. D. Geraedts, M. P. Zaletel, R. S. K. Mong, M. A. Metlitski, A. Vishwanath, and O. I. Motrunich, Science **352**, 197 (2016).
[25] C. Wang and T. Senthil, Phys. Rev. B **94**, 245107 (2016).
[26] G. Murthy and R. Shankar, Phys. Rev. B **93**, 085405 (2016).
[27] M. A. Metlitski and A. Vishwanath, Phys. Rev. B **93**, 245151 (2016).
[28] A. C. Potter, M. Serbyn, and A. Vishwanath, Phys. Rev. X **6**, 031026 (2016).
[29] C. Wang, N. R. Cooper, B. I. Halperin, and A. Stern, Phys. Rev. X **7**, 031029 (2017).
[30] W. Pan, W. Kang, K. W. Baldwin, K. W. West, L. N. Pfeiffer, and D. C. Tsui, Nat. Phys. **13**, 1168 (2017).
[31] G. S. Boebinger, H. L. Stormer, D. C. Tsui, A. M. Chang, J. C. M. Hwang, A. Y. Cho, C. W. Tu, and G. Weimann, Phys. Rev. B **36**, 7919 (1987).
[32] H. C. Manoharan, M. Shayegan, and S. J. Klepper, Phys. Rev. Lett. **73**, 3270 (1994).
[33] B. E. Kane, L. N. Pfeiffer, K. W. West, and C. K. Harnett, Appl. Phys. Lett. **63**, 2132 (1993).
[34] See Supplemental Material at http://link.aps.org/supplemental/10.1103/PhysRevLett.124.156801 for more electronic transport data at other magnetic fields, which includes Ref. [35].
[35] B. Zhang, J. S. Brooks, J. A. A. J. Perenboom, S.-Y. Han, and Q. Qualls, Rev. Sci. Instrum. **70**, 2026 (1999).
[36] H. Goldman and E. Fradkin, Phys. Rev. B **98**, 165137 (2018).
[37] F. C. Zhang and S. D. Sarma, Phys. Rev. B **33**, 2903(R) (1986).
[38] R. L. Willett, H. L. Stormer, D. C. Tsui, A. C. Gossard, and J. H. English, Phys. Rev. B **37**, 8476(R) (1988).
[39] V. Melik-Alaverdian and N. E. Bonesteel, Phys. Rev. B **52**, R17032 (1995).
[40] R. R. Du, H. L. Stormer, D. C. Tsui, L. N. Pfeiffer, and K. W. West, Phys. Rev. Lett. **70**, 2944 (1993).
[41] W. Pan, H. L. Stormer, D. C. Tsui, L. N. Pfeiffer, K. W. Baldwin, and K. W. West, Phys. Rev. B **61**, R5101(R) (2000).
[42] Horst Stormer first pointed out this roughly constant offset in the FQHE activation gap at a conference in Erice, Italy in 2002, and this constant offset is independent of sample type (electron or hole) and mobility.
[43] A. F. Dethlefsen, E. Mariani, H.-P. Tranitz, W. Wegscheider, and R. J. Haug, Phys. Rev. B **74**, 165325 (2006).
[44] G. J. Sreejith, Y. Zhang, and J. K. Jain, Phys. Rev. B **96**, 125149 (2017).
[45] M. Hilke, D. Shahar, S. H. Song, D. C. Tsui, Y. H. Xie, and D. Monroe, Nature (London) **395**, 675 (1998).
[46] V. J. Goldman and M. Shayegan, Surf. Sci. **229**, 10 (1990).
[47] N. Samkharadze, I. Arnold, L. N. Pfeiffer, K. W. West, and G. A. Csáthy, Phys. Rev. B **91**, 081109(R) (2015).
[48] W. Pan, K. W. Baldwin, K. W. West, L. N. Pfeiffer, and D. C. Tsui, Phys. Rev. B **91**, 041301(R) (2015).
[49] C. R. Dean, A. F. Young, P. Cadden-Zimansky, L. Wang, H. Ren, K. Watanabe, T. Taniguchi, P. Kim, J. Hone, and K. L. Shepard, Nat. Phys. **7**, 693 (2011).
[50] B. E. Feldman, B. Krauss, J. H. Smet, and A. Yacoby, Science **337**, 1196 (2012).
[51] F. Amet, A. J. Bestwick, J. R. Williams, L. Balicas, K. Watanabe, T. Taniguchi, and D. Goldhaber-Gordon, Nat. Commun. **6**, 5838 (2015).
[52] A. A. Zibrov, E. M. Spanton, H. Zhou, C. Kometter, T. Taniguchi, K. Watanabe, and A. F. Young, Nat. Phys. **14**, 930 (2018).
[53] B. Hunt, J. D. Sanchez-Yamagishi, A. F. Young, M. Yankowitz, B. J. LeRoy, K. Watanabe, T. Taniguchi, P. Moon, M. Koshino, P. Jarillo-Herrero, and R. C. Ashoori, Science **340**, 1427 (2013).
[54] H. Polshyn, H. Zhou, E. M. Spanton, T. Taniguchi, K. Watanabe, and A. F. Young, Phys. Rev. Lett. **121**, 226801 (2018).
[55] Y. Zeng, J. I. A. Li, S. A. Dietrich, O. M. Ghosh, K. Watanabe, T. Taniguchi, J. Hone, and C. R. Dean, Phys. Rev. Lett. **122**, 137701 (2019).